

Electron state symmetries and optical transitions in semiconductor superlattices: II.

$(\text{GaAs})_m(\text{AlAs})_n$  grown along the [110] and [111] directions

This article has been downloaded from IOPscience. Please scroll down to see the full text article.

1997 J. Phys.: Condens. Matter 9 277

(<http://iopscience.iop.org/0953-8984/9/1/028>)

View [the table of contents for this issue](#), or go to the [journal homepage](#) for more

Download details:

IP Address: 171.66.16.207

The article was downloaded on 14/05/2010 at 06:04

Please note that [terms and conditions apply](#).

## Electron state symmetries and optical transitions in semiconductor superlattices: II. $(\text{GaAs})_m(\text{AlAs})_n$ grown along the $[110]$ and $[111]$ directions

Yu E Kitaev†§, A G Panfilov†§, P Tronc† and R A Evarestov‡

† Laboratoire d'Optique Physique, École Supérieure de Physique et Chimie Industrielles, 10 rue Vauquelin, 75005 Paris, France

‡ St Petersburg State University, Universitetskaya Naberezhnaya 7/9, 199034 St Petersburg, Russia

Received 8 February 1996

**Abstract.** Using the method of induced band representations of space groups, we have performed a complete group-theory analysis of electron state symmetries in  $(\text{GaAs})_m(\text{AlAs})_n$  superlattices grown along the  $[110]$  and  $[111]$  directions. The spin-orbit interaction has been taken into account. The formulae giving, for arbitrary numbers of monolayers  $m$  and  $n$ , the arrangements of atoms over the Wyckoff positions have been obtained. The selection rules for both direct and phonon-assisted optical transitions have been derived. Using results of the group-theory analysis, we predict some variations in the optical transitions when  $m$  and/or  $n$  are varied. We also propose polarized-light optical experiments to establish the detailed electron-band structures of the superlattices.

### 1. Introduction

In a previous paper [1], we performed a complete group-theory analysis of electron state symmetries in  $(\text{GaAs})_m(\text{AlAs})_n$  superlattices (SLs) grown along the  $[001]$  direction. Using both the results of our group-theory analysis and data of various electronic-structure calculations, we proposed polarized-light optical experiments to establish the actual picture of optical transitions in these materials, which can be considered as a new class of artificially grown crystals. We also predicted some variations in the optical spectra upon varying  $m$  and  $n$ . In this paper, we perform a similar analysis for the  $(\text{GaAs})_m(\text{AlAs})_n$  SLs grown along the  $[110]$  and  $[111]$  directions.

To study the optical properties of SLs one should know the complete information about their crystal structure. In section 2, we analyse the dependence of the structure of these materials not only on the growth direction  $[hkl]$  but also on the numbers of monolayers  $m$  and  $n$ .

For each direction of growth, the SLs constitute several single-crystal families specified by different space groups  $G_i$  (the same within each family). These space groups have been found for both the  $[110]$  [2] and  $[111]$  [3] growth directions. Nevertheless, from the crystallographic point of view, the SLs with different numbers of monolayers  $m$  and  $n$  are distinct crystals, even those belonging to the same family, since they differ from each other by the arrangement of atoms over the Wyckoff positions. For the  $[001]$  orientation of layers, the distribution of atoms in the primitive cell has been obtained in our previous

§ Permanent address: A F Ioffe Physical-Technical Institute, Politekhnikeskaya 26, 194021, St Petersburg, Russia.

papers [1, 4, 5]. For other orientations, the arrangement of atoms over the Wyckoff positions in a primitive cell has not been analysed.

The dependence of the SL crystal structure on the numbers of monolayers influences the phonon and electron states in these crystals. For the  $(\text{GaAs})_m(\text{AlAs})_n$  [110] and [111] SLs, the symmetry of phonon states and the corresponding infrared and Raman spectra selection rules have been investigated comprehensively during recent years [2, 3, 6]. A study of the optical anisotropy of the  $(\text{GaAs})_m(\text{AlAs})_n$  [110] SLs has also been reported [7]. No result, according to our knowledge, has been published concerning the symmetry properties of the electron states in SLs grown in the [110] and [111] directions. In section 3, we analyse the electron state symmetries at the symmetry points of the Brillouin zone (BZ).

It is worth noting that the  $(\text{GaAs})_1(\text{AlAs})_1$  SL, i.e., the  $(1 \times 1)$  SL in a short notation, grown along the [110] direction is the same as one grown along the [001] direction. Both structural and symmetry properties of this special SL were analysed in detail in our previous paper [1]. The analysis showed that the  $(1 \times 1)$  SL should be considered as a quite new crystal whose properties have no more in common with those of the parent compounds GaAs and AlAs than the latter do with each other. This SL—as well as the other SLs—should be considered as a crystal with an enlarged unit cell compared with that of the parent materials. Like every crystal, it possesses distinct crystal structure and physical properties including optical ones. Possible polarized-light optical spectra of the  $(\text{GaAs})_1(\text{AlAs})_1$  SL were analysed in [1] as well.

Among the  $(\text{GaAs})_m(\text{AlAs})_n$  SLs, only the  $(1 \times 1)$  [001/110]-grown SL can be considered as a rather equilibrium crystal structure (like GaAs and AlAs) since the  $\text{Ga}_{0.5}\text{Al}_{0.5}\text{As}$  alloy is ordered to the  $(1 \times 1)$  SL under certain conditions of growth [8]. The other SLs can be called ‘non-equilibrium’ crystals for they cannot be grown from a solution or melting under equilibrium growth conditions. Note that the strong range-order ordering and formation of superstructure have also been found in other III–V alloys (see [9] and references therein). This is of interest not only from the thermodynamic point of view but also in respect to many possible applications of short-period SLs such as avalanche devices and optical modulators for integrated optics [10].

In section 4, we derive the selection rules for optical transitions in the  $(\text{GaAs})_m(\text{AlAs})_n$  [110] and [111] SLs and predict which lines could be expected to be observed in polarized optical spectra. Modifications of the spectra, when spin–orbit interaction and/or phonon-assisted processes are taken into account, are analysed.

## 2. Crystal structures of superlattices

The crystal structures of typical representatives of different crystal families are presented in figures 1–5. It should be noted that, to keep the standard settings of space groups for the [110]-grown SLs, the  $y$  axis is chosen to be the growth direction in contrast to [001]-grown and [111]-grown SLs where it is the  $z$ -axis. Every  $(\text{GaAs})_m(\text{AlAs})_n$  SL grown along the [110] direction has an orthorhombic structure, except for the tetragonal  $(1 \times 1)$  SL. In the case of even  $m + n$ , the SLs have simple lattices, whereas the lattices are body-centred when  $m + n$  is odd. The symmetry of the SLs grown along the [111] direction is rhombohedral, the crystal lattice being hexagonal when  $m + n = 3k$  and trigonal when  $m + n \neq 3k$ .

The space groups and formulae giving the atomic arrangements over the Wyckoff positions in the  $(\text{GaAs})_m(\text{AlAs})_n$  SLs grown along the [001] direction are presented elsewhere [1, 4, 5].

We give here similar results obtained for the [110] and [111] orientations of growth axis. These results are summarized in tables 1 and 2, respectively. Here, the numbers

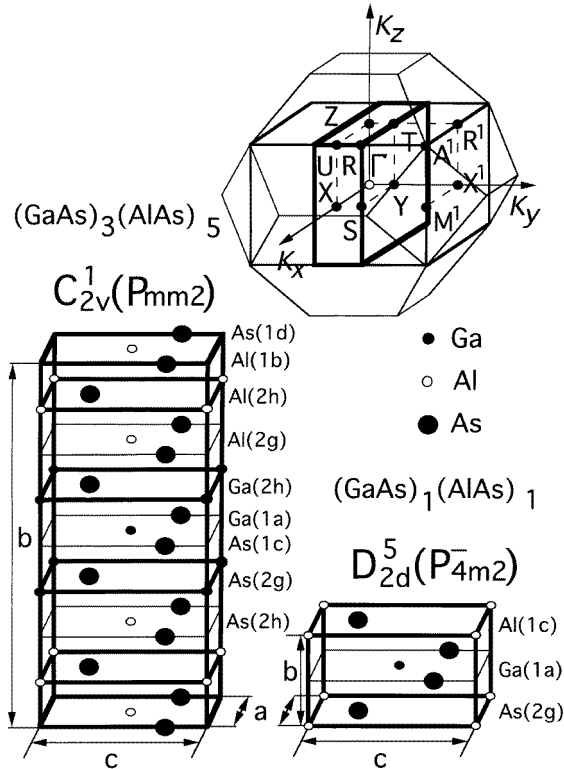


**Figure 1.** The crystal structures of the  $(\text{GaAs})_3(\text{AlAs})_5$  and  $(\text{GaAs})_1(\text{AlAs})_1$  [110]-grown SLs and corresponding BZs drawn by thick and thin lines, respectively. The corresponding points of the BZ of the tetragonal  $(\text{GaAs})_1(\text{AlAs})_1$  [001] SL, being isomorphic to  $(\text{GaAs})_1(\text{AlAs})_1$  [110], are marked by superscript 1.

preceding the chemical element symbols denote the numbers of such atoms at the Wyckoff position shown in parentheses. Analysing tables 1 and 2 one can see that there are several crystal families specified by different space groups, namely  $C_{2v}^1$ ,  $C_{2v}^7$ , and  $C_{2v}^{20}$  among the SLs grown along the [110] direction as well as  $C_{3v}^1$  and  $C_{3v}^5$  among those grown along the [111] direction. In turn, some of the crystal families can be subdivided into several subfamilies specified by non-equivalent types of atomic arrangement over the Wyckoff positions. For example, within the  $C_{2v}^1$  crystal family, there are four SL subfamilies corresponding to odd numbers of both GaAs and AlAs monolayers. The period of atomic arrangements over the Wyckoff positions is equal to four for both  $m$  and  $n$  in this case. The difference between the subfamilies is subtle and results in the variations of occupation numbers of Wyckoff positions with the same site symmetry by atoms of the same type.

The superlattice BZs (SLBZs) of the five space groups are shown in figures 1–5. The SLBZs are embedded in the parent GaAs (AlAs) BZ in order to describe zone foldings. With increasing values of  $m$  and  $n$ , the SLBZs are reduced in the  $k_y$  ([110]-grown SLs) or  $k_z$  ([111]-grown ones) direction. As a result, symmetry points of the parent BZ fold onto symmetry points of a SLBZ. Since, in both parent compounds GaAs and AlAs, the top of the valence band is located at the  $\Gamma$  point of the zinc-blende BZ whereas the bottom of the conduction band is located respectively at the  $\Gamma$  and X points, these are the most important

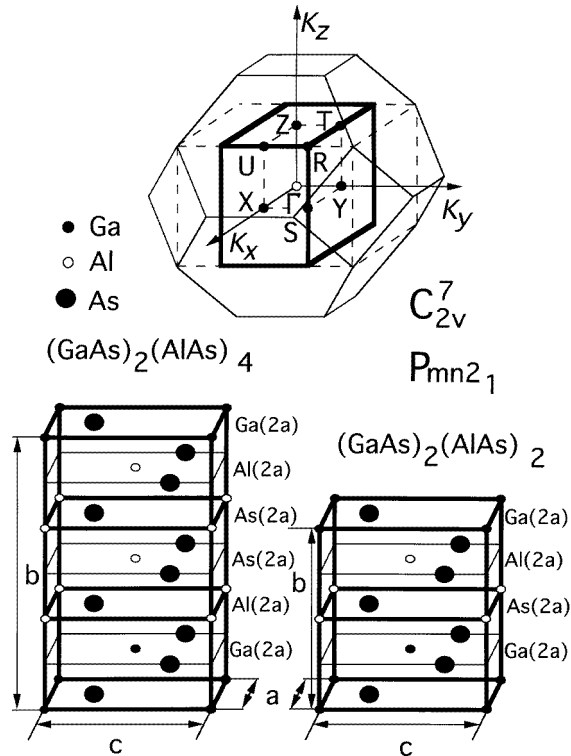


**Figure 2.** The crystal structures and corresponding BZ of the  $(\text{GaAs})_2(\text{AlAs})_4$  and  $(\text{GaAs})_2(\text{AlAs})_2$  [110]-grown SLs.

points. Therefore, it is worth determining which points of the SLBZ they fold onto (the  $\Gamma$  point of the zinc-blende BZ naturally folds onto the  $\Gamma$  point of an SLBZ). Table 3 gives a description of the zone foldings including also the L point of the zinc-blende BZ whose energy in the conduction band is intermediate between those of the  $\Gamma$  and X points in both GaAs and AlAs.

According to most calculations (for references, see e.g. our paper [1]), the conduction-band minimum in the  $(1 \times 1)$  [001]-grown SL is located at the R point of SLBZ, and this is a point which the point L of the GaAs(AlAs) BZ folds onto. In  $(\text{GaAs})_m(\text{AlAs})_n$  [001]-grown SLs with  $m = n$ , one of the lowest conduction-band states is usually located at the M point, which the point X of the parent compounds' BZ folds onto.

In the case of  $m + n = 2k + 1$  for every SL grown in any direction under consideration, the symmetry points of AlAs (GaAs)—except for the  $\Gamma$  point—fold onto surface points of the SLBZ. In contrast, when  $m + n = 2k$ , either X (for the [001] and [110] directions of growth) or L (for the [111] direction) fold onto the  $\Gamma$  point of the SLBZ and there are chances, for some of these SLs, to exhibit a conduction-band minimum at the  $\Gamma$  point with rather low energy.

Very interesting is the case of even-layered [111]-grown SLs. Here, the SLBZ points corresponding to the X point and an L-equivalent point of the GaAs BZ differ by some primitive reciprocal vectors of the SLBZ. That is to say, they fold onto the same point of the SLBZ, namely onto either the point F if  $m + n = 6k \pm 2$  or the point M when  $m + n = 6k$ .

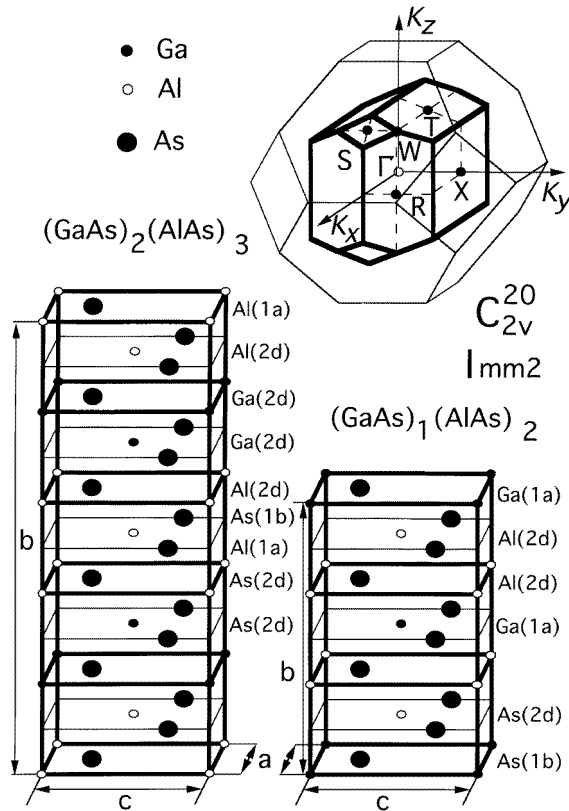


**Figure 3.** The crystal structures and corresponding BZ of the  $(\text{GaAs})_2(\text{AlAs})_3$  and  $(\text{GaAs})_1(\text{AlAs})_2$  [110]-grown SLs.

### 3. Electron state symmetries

The space groups and atomic arrangements being established, we can determine the symmetry of electron states in the  $(\text{GaAs})_m(\text{AlAs})_n$  SLs using the method of induced band representations of space groups [5, 11–14]. This method allows one to establish a symmetry correspondence between extended (Bloch) and localized (Wannier-type) one-electron states in crystals. The electron state symmetries for different SLs are presented in tables 4–8.

The structure of table 4 is the following. Columns 1–4 contain the atomic arrangements over the Wyckoff positions (sites in direct space) given in column 5 together with their coordinates (in units of translation vectors of the crystallographic unit cell) and site symmetry groups. Column 6 contains the Mulliken symbols of those irreducible representations (irreps) of the site symmetry groups for these Wyckoff positions, according to which the localized one-electron wave functions transform, as well as the symbols of double-valued irreps (denoted by a bar over the irrep symbol) in the case where the spin–orbit interaction is taken into account. As already noted in [1], though the Wannier-type orbitals may differ from the corresponding atomic orbitals (s, p, d, etc) they have the same symmetry-transformation properties (i.e. they transform according to the same irreps of a site symmetry group). The remaining columns give the labels of single- and double-valued induced representations in the  $\mathbf{k}$ -basis, with the symbols of  $\mathbf{k}$ -points (wave vectors), their coordinates (in units

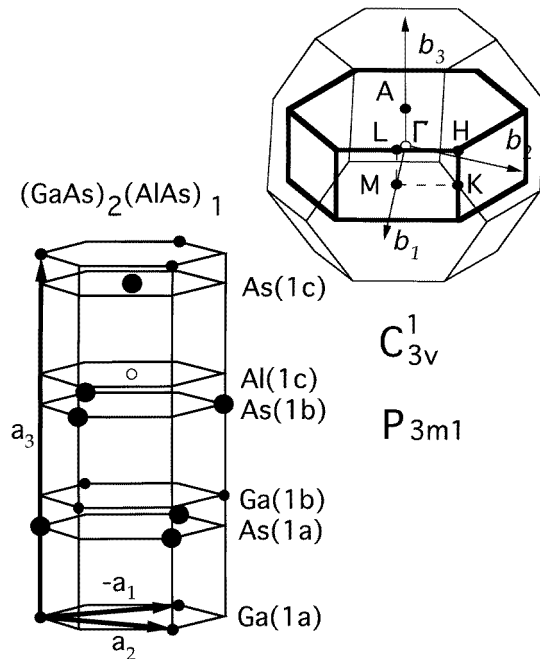


**Figure 4.** The crystal structure and corresponding BZ of the  $(\text{GaAs})_2(\text{AlAs})_1$  [111]-grown SL.

of primitive translations of the reciprocal lattice) and their point groups in rows 1–3 respectively, and the indices of small irreps of little groups in subsequent rows; these determine the symmetries of Bloch states. In this table and in each of the following ones, the labelling of the space group irreps is taken from [15], the labelling of the point group irreps follows [16], and the site points  $q$  are indexed as Wyckoff positions from [17].

The structure of tables 5–8 differs from that of table 4 only by the number of columns containing the atomic arrangements for typical representatives of each SL family (columns 1–4 in table 4, columns 1–6 in table 6, and columns 1–5 in table 7). For the other SL families (tables 5 and 8) all atoms in a primitive cell occupy the same Wyckoff position. This is why atomic arrangements are not given in the latter tables.

As in our previous work [1], we limit ourselves to the  $s$  and  $p$  atomic-like localized states (one  $s$  state and three  $p$  states per atom) since just these functions usually form the uppermost valence-band states and the lowest conduction-band states and, therefore, determine the interband optical transitions. Nevertheless, to describe the lower valence-band states and upper conduction-band ones, the  $d$  states should be also taken into consideration.

Using tables 4–8 one can easily write down the symmetry of the SL band states at symmetry points of the SLBZ and determine which localized states and which atoms in a primitive cell contribute to them.

For example, in the  $(\text{GaAs})_1(\text{AlAs})_2$  [111]-grown SL (table 7), the  $s$  Wannier-type orbital corresponding to the Al atom in 1b Wyckoff position (for short, the  $s$  orbital of Al) induces non-degenerate Bloch states  $\Gamma_1$ ,  $A_1$ ,  $K_2$ ,  $H_2$ ,  $M_1$ , and  $L_1$  (see table 7). Thus, 1 in the column  $\Gamma$  means small irrep  $\Gamma_1$ , 1 in the column A means  $A_1$ , etc. We can also see that  $\Gamma_1$  states are induced by  $s$  and  $p_z$  orbitals of Ga and Al as well as by  $s$  and  $p_z$  orbitals of As, whereas the  $\Gamma_3$  states are formed by  $p_x$  and  $p_y$  orbitals of all atoms. Thus, at the  $\Gamma$

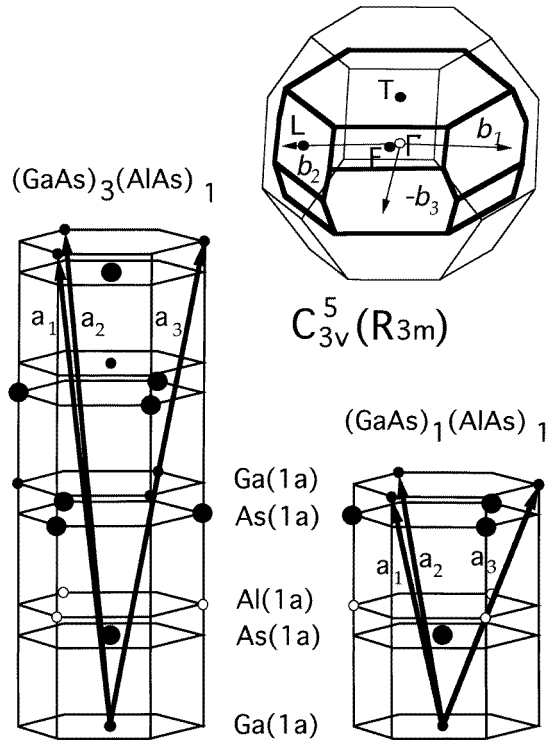


**Figure 5.** The crystal structures and corresponding BZ of the  $(\text{GaAs})_3(\text{AlAs})_1$  and  $(\text{GaAs})_1(\text{AlAs})_1$ , [111]-grown SLs.

point we have six  $\Gamma_1$  and six  $\Gamma_3$  Bloch states resulting from  $s$  and  $p$  localized states (Ga, Al, and As atoms). We can conclude, for example, that the Bloch states induced by  $p_x$  and  $p_y$  orbitals of Ga, Al, and As atoms do not mix at the  $\Gamma$  point with the states induced by  $s$  and  $p_z$  orbitals since they have different symmetries. These results could significantly simplify the numerical calculations of electron-band structures of these materials since for each particular band state we could limit the number of Wannier-type orbitals that should be taken into account. This is especially important if the number of atoms per primitive cell is very large as this is the case for most SLs.

In tables 4–8, the localized states of atoms which occupy low-symmetry positions which do not belong to the so-called Q-set [5] (a small set of points in the real space) induce Bloch states described by composite band representations. This means that they are direct sums of simple irreps, indices of which are presented in corresponding lines of tables 4–8. The simple band representations [5, 14] are induced by irreps of site symmetry groups of only a small set of points in the real space. The band states induced by Wannier-type orbitals corresponding to atoms occupying the Wyckoff positions which do not belong to the Q-set are composite, i.e. they are formed by a combination of simple band representations induced by orbitals of atoms occupying Wyckoff positions from the Q-set.

When the spin-orbit interaction is taken into consideration, the  $s$ ,  $p$ , etc localized orbitals are replaced by the  $|J, m_J\rangle$  orbitals where  $J$  and  $m_J$  are the total angular momentum and its projection. The corresponding double-valued induced representations are also given in tables 4–8. In the case of  $(1 \times 2)$  [111]-grown SL taken as an example, the  $p$ -derived



**Table 1.** Atomic arrangements over the Wyckoff positions in  $(\text{GaAs})_m(\text{AlAs})_n$  [110]-grown SLs.

Space group $C_{2v}^1$ ( $Pmm2$ ), $m = 2k + 1$ , $n = 2l + 1$ ; $m \leq n$			
$m + n = 4i + 2$		$m + n = 4i$	
$m = 4s + 1$	$m = 4s + 3$	$m = 4s + 1$	$m = 4s + 3$
$n = 4t + 1$	$n = 4t + 3$	$n = 4t + 3$	$m = 4t + 1$
1Ga(1a)			
1As(1c)			
1As(1b)		1Al(1b)	
1Al(1d)		1As(1d)	
$(\frac{m+n}{2} - 1)\text{As}(2g)$		$\frac{m+n}{2}\text{As}(2g)$	
$(\frac{m+n}{2} - 1)\text{As}(2h)$		$(\frac{m+n}{2} - 2)\text{As}(2h)$	
$\frac{m-1}{2}\text{Ga}(2g)$	$\frac{m-3}{2}\text{Ga}(2g)$	$\frac{m-1}{2}\text{Ga}(2g)$	$\frac{m-3}{2}\text{Ga}(2g)$
$\frac{m-1}{2}\text{Ga}(2h)$	$\frac{m+1}{2}\text{Ga}(2h)$	$\frac{m-1}{2}\text{Ga}(2h)$	$\frac{m+1}{2}\text{Ga}(2h)$
$\frac{n-1}{2}\text{Al}(2g)$	$\frac{n+1}{2}\text{Al}(2g)$	$\frac{n-3}{2}\text{Al}(2g)$	$\frac{n-1}{2}\text{Al}(2g)$
$\frac{n-1}{2}\text{Al}(2h)$	$\frac{n-3}{2}\text{Al}(2h)$	$\frac{n+1}{2}\text{Al}(2h)$	$\frac{n-1}{2}\text{Al}(2h)$
Space group $C_{2v}^7$ ( $Pmn2_1$ ), $m = 2k$ , $n = 2l$			
$m\text{Ga}(2a)$	$n\text{Al}(2a)$	$(m + n)\text{As}(2a)$	
Space group $C_{2v}^{20}$ ( $Imm2$ ), $m + n = 2i + 1$ ; $m \leq n$			
$m = 2s + 1$		$m = 2s$	
$n = 2t$		$n = 2t + 1$	
1As(1b)			
$(m + n - 1)\text{As}(2d)$			
1Ga(1a)		1Al(1a)	
$(m - 1)\text{Ga}(2d)$		$(n - 1)\text{Al}(2d)$	
$n\text{Al}(2d)$		$m\text{Ga}(2d)$	

$|\frac{3}{2}, \pm\frac{3}{2}\rangle$  localized states of Ga will transform according to double-valued irreps  $\bar{e}_1^{(1)}$  and  $\bar{e}_1^{(2)}$  whereas s-derived  $|\frac{1}{2}, \pm\frac{1}{2}\rangle$ , p-derived  $|\frac{3}{2}, \pm\frac{1}{2}\rangle$ , and  $|\frac{1}{2}, \pm\frac{1}{2}\rangle$  ones will transform according to  $\bar{e}_2$ . As a result, the  $12\Gamma_1 + 6\Gamma_3$  states will become the  $6\Gamma_4 + 6\Gamma_5 + 18\Gamma_6$  ones.

The symmetry correspondence between the Bloch states which transform according to single-valued irreps (without spin-orbit coupling) and those which transform according to the double-valued irreps (with spin-orbit coupling) can be obtained following the procedure described elsewhere [1, 18]. The Bloch state  $D^l$  ( $l = s, p$ ) corresponds to the states which transform according to the double-valued representation  $\bar{D}^l = D^l \times \bar{D}^{1/2}$  where  $\bar{D}^{1/2}$  is the double-valued irrep according to which the spinor function is transformed. For the space groups  $C_{2v}^1$ ,  $C_{2v}^7$ , and  $C_{2v}^{20}$  the spinor function is transformed according to  $\bar{D}^{1/2} = \bar{e}$ , and for the space groups  $C_{3v}^1$  and  $C_{3v}^5$  according to  $\bar{e}_2$ . Decomposing the corresponding direct products of coordinate and spinor parts of the one-electron wave function, we obtain the set of states into which  $D^l$  transforms when spin-orbit interaction is included. At the centre of the BZ, the symmetry correspondence is the following:  $\Gamma_1 \rightarrow \Gamma_6$ ,  $\Gamma_3 \rightarrow \Gamma_4 + \Gamma_5 + \Gamma_6$  (the  $C_{3v}$  groups in question),  $\Gamma_i$  ( $i = 1-4$ )  $\rightarrow \Gamma_5$  (the  $C_{2v}$  groups).

There is a sole double-valued irrep (doubly degenerate) at every symmetry point for the group  $C_{2v}^1$  (e.g.  $\Gamma_5$  at the  $\Gamma$  point, cf table 4). There also exists only one double-valued irrep at points belonging to some symmetry lines of the SLBZ, e.g., the  $\Lambda_5$  irrep for the symmetry

**Table 2.** Atomic arrangements over the Wyckoff positions in  $(\text{GaAs})_m(\text{AlAs})_n$  [111]-grown SLs.

Space group $C_{3v}^1 (P3m1), m+n=3i$		
$m=3s$	$m=3s+1$	$m=3s+2$
$n=3t$	$n=3t+2$	$n=3t+1$
$\frac{m+n}{3}\text{As}(1a)$		
$\frac{m+n}{3}\text{As}(1b)$		
$\frac{m+n}{3}\text{As}(1c)$		
$\frac{m}{3}\text{Ga}(1a)$ $\frac{n}{3}\text{Al}(1a)$	$\frac{m+2}{3}\text{Ga}(1a)$ $\frac{n-2}{3}\text{Al}(1a)$	$\frac{m+1}{3}\text{Ga}(1a)$ $\frac{n-1}{3}\text{Al}(1a)$
$\frac{m}{3}\text{Ga}(1b)$ $\frac{n}{3}\text{Al}(1b)$	$\frac{m-1}{3}\text{Ga}(1b)$ $\frac{n+1}{3}\text{Al}(1b)$	$\frac{m+1}{3}\text{Ga}(1b)$ $\frac{n-1}{3}\text{Al}(1b)$
$\frac{m}{3}\text{Ga}(1c)$ $\frac{n}{3}\text{Al}(1c)$	$\frac{m-1}{3}\text{Ga}(1c)$ $\frac{n+1}{3}\text{Al}(1c)$	$\frac{m-2}{3}\text{Ga}(1c)$ $\frac{n+2}{3}\text{Al}(1c)$
Space group $C_{3v}^5 (R3m), m+n \neq 3i$		
$m\text{Ga}(1a)$	$n\text{Al}(1a)$	$(m+n)\text{As}(1a)$

**Table 3.** The foldings of the symmetry points  $\Gamma$ , X, and L in  $(\text{GaAs})_m(\text{AlAs})_n$  SLs.

Compounds	$m, n$		Symmetry points		
	Space group	Parity			
GaAs (AlAs)	$m+n=1, T_d^2$		$\Gamma$	6X	8L
[001]-grown SLs	$m+n=2i, D_{2d}^5$	$i=2k$	$\Gamma$	$2\Gamma+4M$	$4R+4X$
		$i=2k+1$	$\Gamma$	$2\Gamma+4M$	8R
	$m+n=2i+1, D_{2d}^9$		$\Gamma$	$2M+4X$	8N
[110]-grown SLs	$m=n=1, D_{2d}^5$		$\Gamma$	$2\Gamma+4M$	$4R+4X$
	$m+n=2i, C_{2v}^1, C_{2v}^7$	$i=2k$	$\Gamma$	$2\Gamma+4X$	$4Z+4U$
		$i=2k+1$	$\Gamma$	$2\Gamma+4S$	$4T+4U$
$m+n=2i+1, C_{2v}^{20}$		$\Gamma$	$2X+4R$	$4T+4S$	
[111]-grown SLs	$m+n=3i, C_{3v}^1$	$m+n=2k$	$\Gamma$	6M	$2\Gamma+6M$
		$m+n=2k+1$	$\Gamma$	6M	$2A+6L$
	$m+n \neq 3i, C_{3v}^5$	$m+n=2k$	$\Gamma$	6F	$2\Gamma+6F$
		$m+n=2k+1$	$\Gamma$	6F	$2T+6L$

line  $\Gamma-(\Lambda)-Z$ . In contrast, for other symmetry lines in this SLBZ, there are two double-valued irreps (non-degenerate), which are complex conjugated, e.g.  $\Delta_3$  and  $\Delta_4$  at points of the  $\Gamma-(\Delta)-Y$  line. The complex-conjugated irreps forming a pair correspond to different states with the same energy. This degeneracy is connected with the inversion of time and can be lifted by applying the magnetic field which does not reduce the point symmetry of the system (that is one directed along the symmetry axis). The complex-conjugated irreps can be combined in so-called co-representations (co-reps), which are also called ‘physically irreducible representations’ (doubly degenerate). The corresponding pairs of irreps forming co-reps are given in the captions of tables 5–8. On applying the magnetic field, the states

**Table 4.** Electron state symmetries in  $(\text{GaAs})_m(\text{AlAs})_n$  [110]-grown SLs with the space group  $C_{2v}^1$ .

$m = 1$ $n = 3$	$m = 3$ $n = 3$	$m = 3$ $n = 5$	$m = 5$ $n = 5$	$C_{2v}^1$ ( $Pmm2$ )	$\Gamma$ (000) $C_{2v}$	$X$ ( $\frac{1}{2}00$ ) $C_{2v}$	$Y$ ( $0\frac{1}{2}0$ ) $C_{2v}$	$Z$ ( $00\frac{1}{2}$ ) $C_{2v}$	$S$ ( $\frac{1}{2}\frac{1}{2}0$ ) $C_{2v}$	$T$ ( $0\frac{1}{2}\frac{1}{2}$ ) $C_{2v}$	$U$ ( $\frac{1}{3}0\frac{1}{2}$ ) $C_{2v}$	$R$ ( $\frac{1}{2}\frac{1}{2}\frac{1}{2}$ ) $C_{2v}$
1Ga	1Ga	1Ga	1Ga	$a_1(s; p_z)$	1	1	1	1	1	1	1	1
				1a $b_2(p_y)$	3	3	3	3	3	3	3	3
				(00z) $b_1(p_x)$	4	4	4	4	4	4	4	4
				$C_{2v}$ $\bar{e}$	5	5	5	5	5	5	5	5
1Al	1As	1Al	1As	$a_1(s; p_z)$	1	1	3	1	3	3	1	3
				1b $b_2(p_y)$	3	3	1	3	1	1	3	1
				( $0\frac{1}{2}z$ ) $b_1(p_x)$	4	4	2	4	2	2	4	2
				$C_{2v}$ $\bar{e}$	5	5	5	5	5	5	5	5
1As	1As	1As	1As	$a_1(s; p_z)$	1	4	1	1	4	1	4	4
				1c $b_2(p_y)$	3	2	3	3	2	3	2	2
				( $\frac{1}{2}0z$ ) $b_1(p_x)$	4	1	4	4	1	4	1	1
				$C_{2v}$ $\bar{e}$	5	5	5	5	5	5	5	5
1As	1Al	1As	1Al	$a_1(s; p_z)$	1	4	3	1	2	3	4	2
				1d $b_2(p_y)$	3	2	1	3	4	1	2	4
				( $\frac{1}{2}\frac{1}{2}z$ ) $b_1(p_x)$	4	1	2	4	3	2	1	3
				$C_{2v}$ $\bar{e}$	5	5	5	5	5	5	5	5
			2Ga	$a'(s; p_y, p_z)$	1, 3	1, 3	1, 3	1, 3	1, 3	1, 3	1, 3	1, 3
			2Al	2g $a''(p_x)$	2, 4	2, 4	2, 4	2, 4	2, 4	2, 4	2, 4	2, 4
2As	2As	4As	4As	(0yz) $\bar{e}^{(1)}$	5	5	5	5	5	5	5	5
				$C_s$ $\bar{e}^{(2)}$	5	5	5	5	5	5	5	5
			2Ga	$a'(s; p_y, p_z)$	1, 3	2, 4	1, 3	1, 3	2, 4	1, 3	2, 4	2, 4
			2Al	2h $a''(p_x)$	2, 4	1, 3	2, 4	2, 4	1, 3	2, 4	1, 3	1, 3
2Al	2As	4As	4As	( $\frac{1}{2}yz$ ) $\bar{e}^{(1)}$	5	5	5	5	5	5	5	5
				$C_s$ $\bar{e}^{(2)}$	5	5	5	5	5	5	5	5

**Table 5.** Electron state symmetries in  $(\text{GaAs})_m(\text{AlAs})_n$  [110]-grown SLs with the space group  $C_{2v}^7$  (co-reps:  $X_2 + X_5$ ,  $X_3 + X_4$ ,  $Z_1 + Z_3$ ,  $Z_2 + Z_4$ ,  $U_2 + U_3$ ,  $U_4 + U_5$ ,  $S_2 + S_5$ ,  $S_3 + S_4$ ,  $T_1 + T_3$ ,  $T_2 + T_4$ ,  $R_2 + R_3$ ,  $R_4 + R_5$ ).

$C_{2v}^7$ ( $Pmm2_1$ )	$\Gamma$ (000) $C_{2v}$	$X$ ( $\frac{1}{2}00$ ) $C_{2v}$	$Y$ ( $0\frac{1}{2}0$ ) $C_{2v}$	$Z$ ( $00\frac{1}{2}$ ) $C_{2v}$	$S$ ( $\frac{1}{2}\frac{1}{2}0$ ) $C_{2v}$	$T$ ( $0\frac{1}{2}\frac{1}{2}$ ) $C_{2v}$	$U$ ( $\frac{1}{2}0\frac{1}{2}$ ) $C_{2v}$	$R$ ( $\frac{1}{2}\frac{1}{2}\frac{1}{2}$ ) $C_{2v}$
2a $a'(s; p_y, p_z)$	1, 3	1	1, 3	1, 3	1	1, 3	1	1
(0yz) $a''(p_x)$	2, 4	1	2, 4	2, 4	1	2, 4	1	1
$C_s$ $\bar{e}^{(1)}$	5	2, 4	5	5	2, 4	5	2, 4	2, 4
$\bar{e}^{(2)}$	5	3, 5	5	5	3, 5	5	3, 5	3, 5

described by complex-conjugated irreps are split whereas the states described by doubly degenerate irreps are not.

A very similar situation takes place in the case of the groups  $C_{2v}^{20}$  and  $C_{2v}^7$ . There exists only a doubly degenerate irrep at some symmetry points and symmetry lines (e.g.  $\Gamma_5$ ,  $\Lambda_5$ , etc), whereas, at other symmetry points and lines, there are complex-conjugated irreps, which form co-representations—e.g.  $(S_3, S_4)$ ,  $(\Delta_3, \Delta_4)$ , etc, so, the inclusion of the spin-orbit interaction into consideration simplifies the band picture, reducing to one the

**Table 6.** Electron state symmetries in  $(\text{GaAs})_m(\text{AlAs})_n$  [110]-grown SLs with the space group  $C_{2v}^{20}$  (co-reps:  $S_3 + S_4, R_3 + R_4, T_3 + T_4$ ).

$m = 1$ $n = 2$	$m = 2$ $n = 3$	$m = 1$ $n = 4$	$m = 2$ $n = 5$	$m = 1$ $n = 6$	$m = 3$ $n = 4$	$C_{2v}^{20}$ ( $Imm2$ )	$\Gamma$ (000) $C_{2v}$	X $(\frac{1}{2}\frac{1}{2}\frac{1}{2})$ $C_{2v}$	S $(\frac{1}{2}00)$ $C_s$	R $(0\frac{1}{2}0)$ $C_s$	T $(00\frac{1}{2})$ $C_2$	W $(\frac{1}{4}\frac{1}{4}\frac{1}{4})$ $C_2$
1Ga	1Al	1Ga	1Al	1Ga	1Ga	1a	$a_1(s; p_z)$	1	1	1	1	1
						(00z)	$b_2(p_y)$	3	3	1	2	2
						$C_{2v}$	$b_1(p_x)$	4	4	2	1	2
						$\bar{e}$	$\bar{e}$	5	5	3, 4	3, 4	3, 4
1As	1As	1As	1As	1As	1As	1b	$a_1(s; p_z)$	1	1	1	1	2
						$(0\frac{1}{2}z)$	$b_2(p_y)$	3	3	1	2	1
						$C_{2v}$	$b_1(p_x)$	4	4	2	1	1
						$\bar{e}$	$\bar{e}$	5	5	3, 4	3, 4	3, 4
	2Ga		2Ga		2Ga	2d	$a'(s; p_y, p_z)$	1, 3	1, 3	1, 1	1, 2	1, 2
2Al	2Al	4Al	4Al	6Al	4Al	(0yz)	$a'(p_x)$	2, 4	2, 4	2, 2	1, 2	1, 2
2As	4As	4As	6As	6As	6As	$C_s$	$\bar{e}^{(1)}$	5	5	3, 4	3, 4	3, 4
							$\bar{e}^{(2)}$	5	5	3, 4	3, 4	3, 4

**Table 7.** Electron state symmetries in  $(\text{GaAs})_m(\text{AlAs})_n$  [111]-grown SLs with the space group  $C_{3v}^1$  (co-reps:  $\Gamma_4 + \Gamma_5, A_4 + A_5, M_3 + M_4, L_3 + L_4$ ).

$m = 1$ $n = 2$	$m = 2$ $n = 1$	$m = 3$ $n = 3$	$m = 1$ $n = 5$	$m = 2$ $n = 4$	$C_{3v}^1$ ( $P\bar{3}m1$ )	$\Gamma$ (000) $C_{3v}$	A $(00\frac{1}{2})$ $C_{3v}$	K $(\frac{1}{3}\frac{1}{3}0)$ $C_3$	H $(\frac{1}{3}\frac{1}{3}\frac{1}{2})$ $C_3$	M $(\frac{1}{2}00)$ $C_s$	L $(\frac{1}{2}0\frac{1}{2})$ $C_s$
		1Ga	1Ga	1Ga		$a_1(s; p_z)$	1	1	1	1	1
1Ga	1Ga	1Al	1Al	1Al		$e(p_x, p_y)$	3	3	2, 3	2, 3	1, 2
1As	1As	2As	2As	2As	1a	$\bar{e}_1^{(1)}$	4	4	5	5	4
					(00z)	$\bar{e}_1^{(2)}$	5	5	5	5	3
					$C_{3v}$	$\bar{e}_2$	6	6	4, 6	4, 6	3, 4
		1Ga		1Ga		$a_1(s; p_z)$	1	1	2	2	1
1Al	1Ga	1Al	2Al	1As		$e(p_x, p_y)$	3	3	1, 3	1, 3	1, 2
1As	1As	2As	2As	2As	1b	$\bar{e}_1^{(1)}$	4	4	6	6	4
					$(\frac{1}{3}\frac{2}{3}z)$	$\bar{e}_1^{(2)}$	5	5	6	6	3
					$C_{3v}$	$\bar{e}_2$	6	6	4, 5	4, 5	3, 4
		1Ga				$a_1(s; p_z)$	1	1	3	3	1
1Al	1Al	1Al	2Al	2Al		$e(p_x, p_y)$	3	3	1, 2	1, 2	1, 2
1As	1As	2As	2As	2As	1c	$\bar{e}_1^{(1)}$	4	4	4	4	4
					$(\frac{2}{3}\frac{1}{3}z)$	$\bar{e}_1^{(2)}$	5	5	4	4	3
					$C_{3v}$	$\bar{e}_2$	6	6	5, 6	5, 6	3, 4

number of representations describing electron state symmetries at a given point of the SLBZ of [110]-grown SLs.

More complicated is the case of the [111]-grown SLs. When the spin-orbit coupling is taken into account, even at the  $\Gamma$  point, there are both states that are described by doubly degenerate irreps,  $\Gamma_6$ , and states which can be described by co-representations,  $(\Gamma_4, \Gamma_5)$ . Only the latter will split on applying the magnetic field, not reducing the  $C_{3v}$  symmetry. In addition, it is to be noticed that, for [111]-grown SLs, there are two doubly degenerate  $\Gamma_6$  states, one being derived from the  $\Gamma_1$  state and the other originating from the doubly degenerate  $\Gamma_3$  one.

**Table 8.** Electron state symmetries in  $(\text{GaAs})_m(\text{AlAs})_n$  [111]-grown SLs with the space group  $C_{3v}^5$  ( $\mathbf{a} = \mathbf{a}_1 + \mathbf{a}_2 + \mathbf{a}_3$ ; co-reps:  $\Gamma_4 + \Gamma_5$ ,  $T_4 + T_5$ ,  $L_3 + L_4$ ,  $F_3 + F_4$ ).

$C_{3v}^5 (R3m)$		$\Gamma$	$T$	$L$	$F$
		(000) $C_{3v}$	$(\frac{1}{2} \frac{1}{2} \frac{1}{2})$ $C_{3v}$	$(0 \frac{1}{2} 0)$ $C_s$	$(\frac{1}{2} \frac{1}{2} 0)$ $C_s$
1a	$a(s; p_z)$	1	1	1	1
$(\nu a)$	$e(p_x, p_y)$	3	3	1, 2	1, 2
$C_{3v}$	$\bar{e}_1^{(1)}$	4	4	3	3
	$\bar{e}_1^{(2)}$	5	5	4	4
	$\bar{e}_2$	6	6	3, 4	3, 4

**Table 9.** The correspondence between the  $\Gamma$  irreps of different space groups describing bulk GaAs (AlAs) and SLs grown along different directions. For the cubic  $T_d$  symmetry, the Miller–Love [15] notation is used, the commonly used labelling being given in parentheses.

$T_d$	$D_{2d}$	$C_{2v}$	$C_{3v}$	$D_{2d}$	$C_{2v}$
GaAs(AlAs)	[001]	[110]	[111]	[001]	[110]
Single-valued irreps					
$\Gamma_1 (\Gamma_1)$	$\Gamma_1$	$\Gamma_1$	$\Gamma_1$	$\Gamma_1$	$\Gamma_1$
$\Gamma_2 (\Gamma_2)$	$\Gamma_4$	$\Gamma_2$	$\Gamma_2$	$\Gamma_2$	$\Gamma_1$
$\Gamma_3 (\Gamma_{12})$	$\Gamma_1 + \Gamma_4$	$\Gamma_1 + \Gamma_2$	$\Gamma_3$	$\Gamma_3$	$\Gamma_2$
$\Gamma_4 (\Gamma'_{15})$	$\Gamma_2 + \Gamma_5$	$\Gamma_1 + \Gamma_3 + \Gamma_4$	$\Gamma_1 + \Gamma_3$	$\Gamma_4$	$\Gamma_2$
$\Gamma_5 (\Gamma'_{25})$	$\Gamma_3 + \Gamma_5$	$\Gamma_2 + \Gamma_3 + \Gamma_4$	$\Gamma_2 + \Gamma_3$	$\Gamma_5$	$\Gamma_3 + \Gamma_4$
Double-valued irreps					
$\Gamma_6 (\Gamma_7)$	$\Gamma_6$	$\Gamma_5$	$\Gamma_6$	$\Gamma_6$	$\Gamma_5$
$\Gamma_7 (\Gamma_6)$	$\Gamma_7$	$\Gamma_5$	$\Gamma_6$	$\Gamma_7$	$\Gamma_5$
$\Gamma_8 (\Gamma_8)$	$\Gamma_6 + \Gamma_7$	$\Gamma_5 + \Gamma_5$	$\Gamma_4 + \Gamma_5 + \Gamma_6$		

At lower symmetry points, the bands that are degenerated at symmetry points of SLBZ can split. For the SLs with the space groups  $C_{2v}^1$ , such splitting can exist—although only in the presence of the magnetic field—along the symmetry lines  $\Gamma$ –( $\Delta$ )–Y–(C)–S–(D)–X–( $\Sigma$ )– $\Gamma$  and Z–(B)–T–(E)–R–(P)–U–(A)–Z whereas it is absent along the  $\Gamma$ –( $\Lambda$ )–Z, Y–(H)–T, X–(G)–U, and S–(Q)–R symmetry lines. Note that bands also remain degenerate along the symmetry line  $\Gamma$ –Z in the other [110]- and [111]-grown SLs.

One can obtain the correspondence between the irreps of different space groups. Physically, such a correspondence reflects a similarity of symmetry properties of electron states in different  $(\text{GaAs})_m(\text{AlAs})_n$  SLs and GaAs(AlAs) crystals. It is reasonable to consider the correspondence when the alteration of the system symmetry slightly changes symmetry properties of localized states. Alteration of such a kind can appear either under small perturbation (e.g. under pressure/mismatching) or on replacing certain atoms in a lattice (transformation of one SL into another).

The relations between the irreps of a main group and those of its subgroup can be established by subducing the irreps of the group on the subgroup. By doing this, some of the irreps remain irreducible whereas the others become reducible representations. Decomposing the latter over the irreps of the subgroup, one obtains a sum of irreps of the subgroup, which correspond to the irrep of the main group.

The correspondence is presented in table 9 where, as the main group, either the  $T_d$  group (the left part of table 9) or the  $D_{2d}$  group (the right part) is taken. One can see

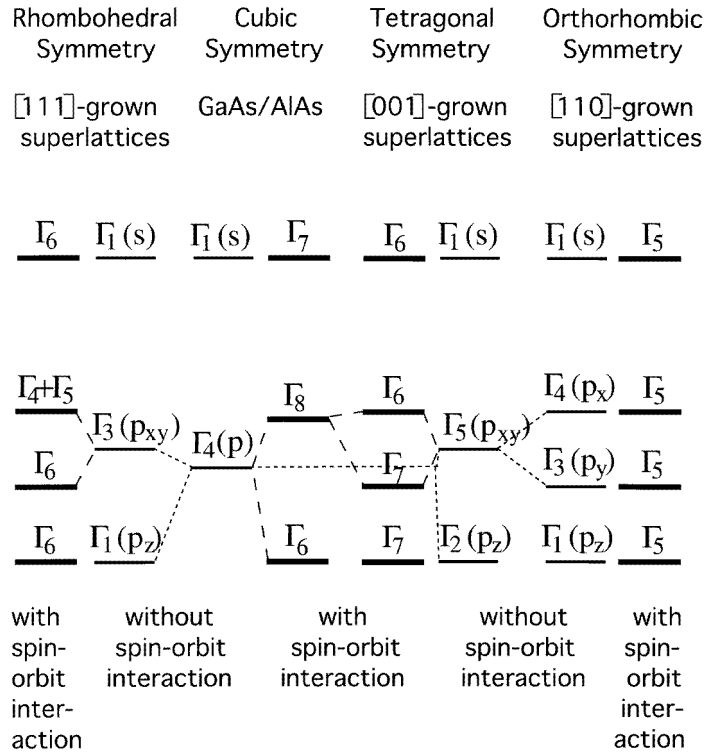


**Figure 6.** The correspondence between the band states at the centre of the BZ of  $(\text{GaAs})_m(\text{AlAs})_n$  SLs originating from the bottom of the conduction band and the top of the valence band of bulk GaAs (AlAs). The co-rep  $\Gamma_4 + \Gamma_5$  describes a degenerate state of the  $(\text{GaAs})_m(\text{AlAs})_n$  [111] SL.

that, on lowering the symmetry from a cubic  $T_d$  (GaAs or AlAs) down to a tetragonal  $D_{2d}$  (the [001]-grown SLs; pressure along a fourth-order axis), the  $\Gamma_4$  states ( $\Gamma_{15}$  states in usual notation) split into  $\Gamma_2$  and  $\Gamma_5$  ones (note different notations of irreps within different groups). When the spin-orbit interaction is taken into account, this corresponds to the splitting of  $\Gamma_8$  states into  $\Gamma_6$  and  $\Gamma_7$  ones. On further lowering the symmetry down to an orthorhombic  $C_{2v}$  (the [110]-grown SLs; pressure along a  $C_2$  axis), the  $\Gamma_5$  states split into  $\Gamma_3 + \Gamma_4$  ones. Figure 6 shows the symmetry modification of the lowest conduction-band and the highest valence-band states at the centre of the BZ when the system symmetry changes.

#### 4. Optical-transition selection rules

The selection rules for optical transitions follow from the symmetry restrictions imposed on matrix elements of transitions from an initial ( $i$ ) electron state to a final ( $f$ ) one. The transitions can be allowed [1] between those pairs of electron states  $D^f$  and  $D^i$  for which the Kronecker product contains the rep with  $\mathbf{k} = \mathbf{0}$ . In tables 10–13, we present the  $\mathbf{k} = \mathbf{0}$  parts of Kronecker products of irreps corresponding to various combinations of initial and final electron states at the symmetry points of the SLBZ. For example, within the space group

**Table 10.** Selection rules for direct optical transitions in  $(\text{GaAs})_m(\text{AlAs})_n$  [110] SLs with the space group  $C_{2v}^1$  for the symmetry points  $D = \Gamma, X, Y, Z, S, T, U$ , and  $R$ .

	$\Gamma_1$	$\Gamma_2$	$\Gamma_3$	$\Gamma_4$	Allowed polarizations
Single-valued irreps					
$D_i \times D_i$ ( $i = 1-4$ )	+				$z$
$D_1 \times D_2, D_3 \times D_4$		+			forbidden
$D_1 \times D_3, D_2 \times D_4$			+		$y$
$D_1 \times D_4, D_2 \times D_3$				+	$x$
Double-valued irreps (with spin-orbit interaction included)					
$D_5 \times D_5$	+	+	+	+	$x, y, z$

**Table 11.** Selection rules for direct optical transitions in  $(\text{GaAs})_m(\text{AlAs})_n$  [110] SLs with the space group  $C_{2v}^7$ .

	$\Gamma_1$	$\Gamma_2$	$\Gamma_3$	$\Gamma_4$	Allowed polarizations
Single-valued irreps					
$D = \Gamma, Y$					
$D_i \times D_i$ ( $i = 1-4$ )	+				$z$
$D_1 \times D_2, D_3 \times D_4$		+			forbidden
$D_1 \times D_3, D_2 \times D_4$			+		$y$
$D_1 \times D_4, D_2 \times D_3$				+	$x$
$D = Z, T$					
$D_i \times D_i$ ( $i = 1-4$ )			+		$y$
$D_1 \times D_2, D_3 \times D_4$				+	$x$
$D_1 \times D_3, D_2 \times D_4$	+				$z$
$D_1 \times D_4, D_2 \times D_3$		+			forbidden
$D = X, S, U, R$					
$D_1 \times D_1$	+	+	+	+	$x, y, z$
Double-valued irreps (with spin-orbit interaction included)					
$D = \Gamma, Y, Z, T$					
$D_5 \times D_5$	+	+	+	+	$x, y, z$
$D = X, S$					
$D_i \times D_i$ ( $i = 2-5$ )				+	$x$
$D_2 \times D_3, D_4 \times D_5$			+		$y$
$D_2 \times D_4, D_3 \times D_5$		+			forbidden
$D_2 \times D_5, D_3 \times D_4$	+				$z$
$D = U, R$					
$D_i \times D_i$ ( $i = 2-5$ )		+			forbidden
$D_2 \times D_3, D_4 \times D_5$	+				$z$
$D_2 \times D_4, D_3 \times D_5$				+	$x$
$D_2 \times D_5, D_3 \times D_4$			+		$y$

$C_{2v}^{20}$ ,  $R_1 \times R_2 = \Gamma_2 + \Gamma_3 + X_2 + X_3$ , and + in the columns  $\Gamma_2$  and  $\Gamma_3$  means that these irreps form part of the direct product. The transitions are allowed between those pairs of states for which Kronecker products have irreps in common with the vector representation. For the space groups  $C_{2v}^1$ ,  $C_{2v}^7$ , and  $C_{2v}^{20}$ , the vector representation is  $D^v = \Gamma_1(z) + \Gamma_3(y) + \Gamma_4(x)$ ;

**Table 12.** Selection rules for direct optical transitions in  $(\text{GaAs})_m(\text{AlAs})_n$  [110] SLs with the space group  $C_{2v}^{20}$ .

	$\Gamma_1$	$\Gamma_2$	$\Gamma_3$	$\Gamma_4$	Allowed polarizations
Single-valued irreps					
D = $\Gamma$ , X					
$D_i \times D_i$ ( $i = 1-4$ )	+				z
$D_1 \times D_2, D_3 \times D_4$		+			forbidden
$D_1 \times D_3, D_2 \times D_4$			+		y
$D_1 \times D_4, D_2 \times D_3$				+	x
$S_1 \times S_1, S_2 \times S_2$	+		+		y, z
$S_1 \times S_2$		+		+	x
$R_1 \times R_1, R_2 \times R_2$	+			+	x, z
$R_1 \times R_2$		+	+		y
D = T, W					
$D_1 \times D_1, D_2 \times D_2$	+	+			z
$D_1 \times D_2$			+	+	x, y
Double-valued irreps (with spin-orbit interaction included)					
$\Gamma_5 \times \Gamma_5, X_5 \times X_5$	+	+	+	+	x, y, z
$S_3 \times S_3, S_4 \times S_4$		+		+	x
$S_3 \times S_4$	+		+		y, z
$R_3 \times R_3, R_4 \times R_4$		+	+		y
$R_3 \times R_4$	+			+	x, z
$T_3 \times T_3, T_4 \times T_4, W_3 \times W_4$			+	+	x, y
$W_3 \times W_3, W_4 \times W_4, T_3 \times T_4$	+	+			z

for the space groups  $C_{3v}^1$  and  $C_{3v}^5$ , it is  $D^v = \Gamma_1(z) + \Gamma_3(x, y)$ . Thus, the optical transition between the states  $R_1$  and  $R_2$  taken above as an example is allowed in the  $y$  polarization and forbidden in the  $x$  and  $z$  polarizations. For co-reps  $D_i + D_j$ , the corresponding Kronecker products of separate irreps  $D_i \times D_i = D_i \times (D_j)^*$  and  $D_i \times D_j = D_i \times (D_i)^*$  describe the transitions between the states  $D_i$  and  $D_j$ , and  $D_i$  and  $D_i$ , respectively.

The upper parts of tables 10–13 give the selection rules without account of spin-orbit coupling. The latter mixes states and smooths the difference between them, especially for the [110]-grown SLs. When the spin-orbit interaction is taken into consideration, all direct optical transitions are completely allowed between the  $\Gamma$  states in the [110]-grown SLs (cf the last line of table 10). This is another manifestation of the fact that these band states do not differ from each other in symmetry (see section 3). However, in actual SLs, the spin-orbit interaction is not extremely strong. This is why, when analysing optical spectra, it is worth taking into account the genesis of states, that is the symmetry correspondence between Bloch states with and without this interaction, and modification of selection rules. For example, a transition between two  $\Gamma_1$  states is allowed only in the  $z$  polarization, and the transition between  $\Gamma_5$  states originating from them is allowed in the  $x$  and  $y$  polarizations as well. So, in actual  $(\text{GaAs})_m(\text{AlAs})_n$  [110]-grown SLs, all the direct  $\Gamma$ – $\Gamma$  optical transitions should be observed in the polarized spectra, though some of them being allowed in certain polarizations only due to the spin-orbit interaction.

As to other points of the BZ of [110]-grown  $(\text{GaAs})_m(\text{AlAs})_n$  SLs and every BZ point of [111]-grown ones, the picture is not so simple. If both the spin-orbit interaction is taken into account and the magnetic field is absent, some of the band states can be



**Table 13.** Selection rules for direct optical transitions in  $(\text{GaAs})_m(\text{AlAs})_n$  [110] SLs with the space group  $C_{3v}^1$  (the  $\Gamma$ , A, H, K, L, and M symmetry points) and  $C_{3v}^5$  (the  $\Gamma$ , T, L, and F symmetry points of the SLBZ).

	$\Gamma_1$	$\Gamma_2$	$\Gamma_3$	Allowed polarizations
<b>Single-valued irreps</b>				
D = $\Gamma$ , T, A				
$D_1 \times D_1, D_2 \times D_2$	+			z
$D_1 \times D_2$		+		forbidden
$D_1 \times D_3, D_2 \times D_3$			+	x, y
$D_3 \times D_3$	+	+	+	x, y, z
D = H, K				
$D_i \times D_i$ ( $i = 1-3$ )	+	+		z
$D_1 \times D_2, D_1 \times D_3, D_2 \times D_3$			+	x, y
D = L, F, M				
$D_1 \times D_1, D_2 \times D_2$	+		+	x, y, z
$D_1 \times D_2$		+	+	x, y
<b>Double-valued irreps (with spin-orbit interaction included)</b>				
D = $\Gamma$ , T, A				
$D_4 \times D_4, D_5 \times D_5$		+		forbidden
$D_4 \times D_5$	+			z
$D_4 \times D_6, D_5 \times D_6$			+	x, y
$D_6 \times D_6$	+	+	+	x, y, z
D = H, K				
$D_i \times D_i$ ( $i = 4-6$ )	+	+		z
$D_4 \times D_5, D_4 \times D_6, D_5 \times D_6$			+	x, y
D = L, M, F				
$D_3 \times D_4$	+		+	x, y, z
$D_3 \times D_3, D_4 \times D_4$		+	+	x, y

described by co-reps, having the same energies. The selection rules for the transitions between such combined states can be easily obtained since the co-reps are direct sums of complex-conjugated counterparts. The magnetic field lifts the degeneracy related to the time inversion. As a result, states which are described by complex-conjugated irreps may have different energies and be involved in transitions with different selection rules (tables 11–13).

For the  $(\text{GaAs})_m(\text{AlAs})_n$  [111]-grown SLs, taking into account the symmetry correspondence between single- and double-valued irreps, we can obtain a relation between the selection rules when the spin-orbit interaction is taken into consideration (lower parts of table 13) and those when it is not (upper part). This correspondence is schematically presented in figure 7. From table 13, it follows that, whereas the transition between two  $\Gamma_6$  states is completely allowed when both of them are derived from the  $\Gamma_3$  states, the oscillator strength of a transition between two  $\Gamma_6$  states originated either from the  $\Gamma_1$  and  $\Gamma_3$  states or from two  $\Gamma_1$  states depends on the intermixing of  $\Gamma_1$  and  $\Gamma_3$  states by the spin-orbit interaction, that is on the strength of the latter. When the interaction is taken into account, a  $\Gamma_1$ – $\Gamma_1$ -originated transition (allowed in the  $z$  polarization) becomes weakly allowed in the  $x$  and  $y$  polarizations, and the  $\Gamma_1$ – $\Gamma_3$ -originated one (allowed in the  $x$  and  $y$  polarizations) does in the  $z$  polarization. These peculiarities of different  $\Gamma_6$  states can help to interpret the

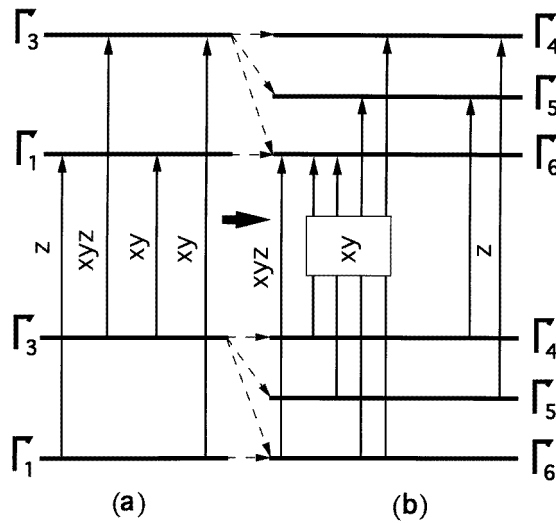


**Figure 7.** The modification of allowed direct optical transitions on including spin-orbit interaction (the space groups  $C_{3v}^1$  and  $C_{3v}^5$ ): (a) without spin-orbit interaction; (b) including spin-orbit interaction.

optical spectra. Additional information can be obtained in experiments with the magnetic field, not reducing the system symmetry. The latter does not split double-degenerated  $\Gamma_6$  states, whereas ‘physically degenerated’ ( $\Gamma_4$ ,  $\Gamma_5$ ) states can split, multiplying the number of direct optical transitions.

Besides direct optical transitions, the phonon-assisted ones may be of importance. In the same manner, as was done for the  $(\text{GaAs})_m(\text{AlAs})_n$  [001]-grown SLs [1], we can obtain the selection rules for phonon-assisted optical transitions. For the [001] short-period SLs as well as for both parent compounds, the uppermost valence-band states at the  $\Gamma$  point are about 1 eV higher in energy than the states at the other symmetry points [1]. One can expect that this will be the case for the  $(\text{GaAs})_m(\text{AlAs})_n$  [110]- and [111]-grown SLs. Therefore, due to such a large difference in energy, for the light-absorption processes, one can neglect the transitions via the virtual valence-band states at symmetry points with wave vector  $\mathbf{k} \neq \mathbf{0}$ . This is why we consider both initial and virtual electron states belonging to the same  $\mathbf{k} = \mathbf{0}$  ( $\Gamma$  states).

The results are presented in tables 14 and 15. For [110]-grown SLs when spin-orbit interaction is taken into account, not only are all transitions between initial and virtual  $\Gamma$  states allowed (since all direct  $\Gamma$ - $\Gamma$  optical transitions are completely allowed) but, moreover, any phonon (with an appropriate wave vector) can participate in transitions between virtual and final states. When neglecting the spin-orbit interaction, a phonon-assisted process is allowed if the transition between initial and virtual states is allowed. The only question is, therefore, which of the phonons participates in the transition. Table 14 gives these assisting phonons. Table 15 presents the selection rules for the  $(\text{GaAs})_m(\text{AlAs})_n$  [111]-grown SLs.

The transitions involving optical phonons with  $\mathbf{k} = \mathbf{0}$ , which are of special importance when two conduction bands have energies close one to the other at the  $\Gamma$  point, are also included in tables 13–15. When two valence bands are close to each other at the centre of the

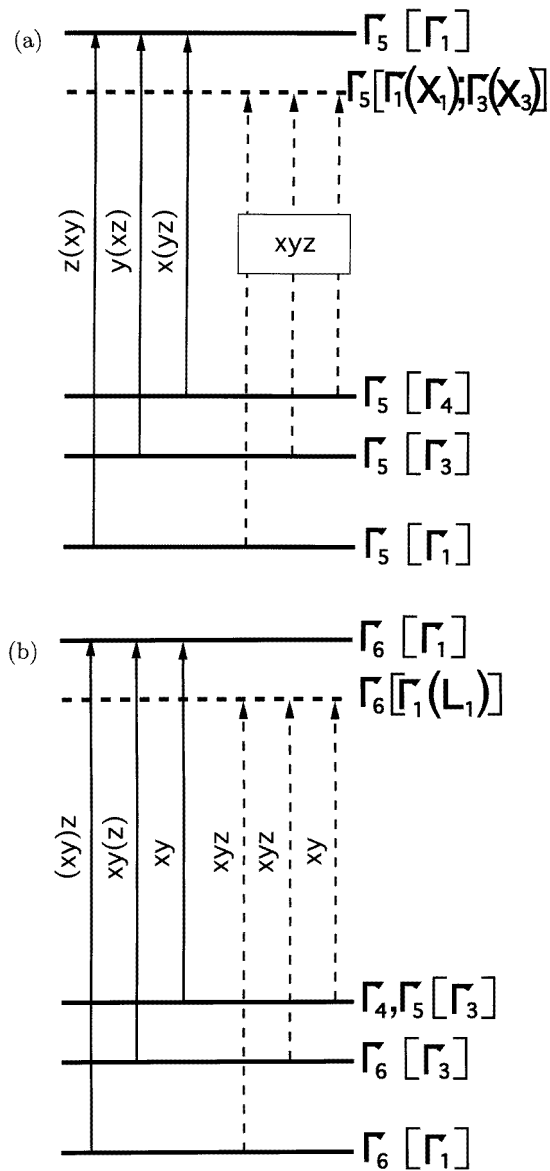


**Figure 8.** Possible energy-level diagrams and dipole-allowed direct optical transitions in  $(\text{GaAs})_m(\text{AlAs})_n$  superlattices: (a) [110] grown; (b) [111] grown. The  $\Gamma$  states of SLs not originating from  $\Gamma$  states of the parent materials and corresponding optical transitions involving these states are shown by dashed lines. The states without spin-orbit interaction are given in square brackets; the corresponding folded bulk states are shown in parentheses.

SLBZ, there may also exist  $\Gamma$ -phonon-assisted optical transitions via virtual valence-band states, the selection rules being similar to the ones given in the tables.

As a result of the above analysis, we can roughly outline the picture of interband transitions in  $(\text{GaAs})_m(\text{AlAs})_n$  [110]- and [111]-grown SLs. Figure 8 schematically presents energy-level diagrams for these SLs. In order not to overload the diagrams, only states at

**Table 14.** Selection rules and assisting phonons for indirect optical transitions in  $(GaAs)_m(AlAs)_n$  [110] SLs with the space group  $C_{2v}^1$ ,  $C_{2v}^7$ , and  $C_{2v}^{20}$ .

Initial state (valence band)	Virtual state (conduction band)	Allowed polarizations	Final states									
			$D = \Gamma, Y, Z, T$ ( $C_{2v}^1, C_{2v}^7$ ) $D = X, S, U, R$ ( $C_{2v}^1$ ) $D = \Gamma, X$ ( $C_{2v}^{20}$ )				$D = X, S, U, R$ ( $C_{2v}^7$ )		$D = S, R$ ( $C_{2v}^{20}$ )		$D = T, W$ ( $C_{2v}^{20}$ )	
			Without the spin-orbit interaction									
			D <sub>1</sub>	D <sub>2</sub>	D <sub>3</sub>	D <sub>4</sub>	D <sub>1</sub>	D <sub>1</sub>	D <sub>2</sub>	D <sub>1</sub>	D <sub>2</sub>	
Assisting phonons												
$\Gamma_1$	$\Gamma_1$	$z$	D <sub>1</sub>	D <sub>2</sub>	D <sub>3</sub>	D <sub>4</sub>	D <sub>1</sub>	D <sub>1</sub>	D <sub>2</sub>	D <sub>1</sub>	D <sub>2</sub>	
	$\Gamma_2$	forbidden	—	—	—	—	—	—	—	—	—	
	$\Gamma_3$	$y$	D <sub>3</sub>	D <sub>4</sub>	D <sub>1</sub>	D <sub>2</sub>	D <sub>1</sub>	D <sub>2</sub>	D <sub>1</sub>	D <sub>2</sub>	D <sub>1</sub>	
	$\Gamma_4$	$x$	D <sub>4</sub>	D <sub>3</sub>	D <sub>2</sub>	D <sub>1</sub>	D <sub>1</sub>	D <sub>1</sub>	D <sub>2</sub>	D <sub>2</sub>	D <sub>1</sub>	
$\Gamma_2$	$\Gamma_1$	forbidden	—	—	—	—	—	—	—	—	—	
	$\Gamma_2$	$z$	D <sub>2</sub>	D <sub>1</sub>	D <sub>4</sub>	D <sub>3</sub>	D <sub>1</sub>	D <sub>2</sub>	D <sub>1</sub>	D <sub>1</sub>	D <sub>2</sub>	
	$\Gamma_3$	$x$	D <sub>3</sub>	D <sub>4</sub>	D <sub>1</sub>	D <sub>2</sub>	D <sub>1</sub>	D <sub>2</sub>	D <sub>1</sub>	D <sub>2</sub>	D <sub>1</sub>	
	$\Gamma_4$	$y$	D <sub>4</sub>	D <sub>3</sub>	D <sub>2</sub>	D <sub>1</sub>	D <sub>1</sub>	D <sub>1</sub>	D <sub>2</sub>	D <sub>2</sub>	D <sub>1</sub>	
$\Gamma_3$	$\Gamma_1$	$y$	D <sub>1</sub>	D <sub>2</sub>	D <sub>3</sub>	D <sub>4</sub>	D <sub>1</sub>	D <sub>1</sub>	D <sub>2</sub>	D <sub>1</sub>	D <sub>2</sub>	
	$\Gamma_2$	$x$	D <sub>2</sub>	D <sub>1</sub>	D <sub>4</sub>	D <sub>3</sub>	D <sub>1</sub>	D <sub>2</sub>	D <sub>1</sub>	D <sub>1</sub>	D <sub>2</sub>	
	$\Gamma_3$	$z$	D <sub>3</sub>	D <sub>4</sub>	D <sub>1</sub>	D <sub>2</sub>	D <sub>1</sub>	D <sub>2</sub>	D <sub>1</sub>	D <sub>2</sub>	D <sub>1</sub>	
	$\Gamma_4$	forbidden	—	—	—	—	—	—	—	—	—	
$\Gamma_4$	$\Gamma_1$	$x$	D <sub>1</sub>	D <sub>2</sub>	D <sub>3</sub>	D <sub>4</sub>	D <sub>1</sub>	D <sub>1</sub>	D <sub>2</sub>	D <sub>1</sub>	D <sub>2</sub>	
	$\Gamma_2$	$y$	D <sub>2</sub>	D <sub>1</sub>	D <sub>4</sub>	D <sub>3</sub>	D <sub>1</sub>	D <sub>2</sub>	D <sub>1</sub>	D <sub>1</sub>	D <sub>2</sub>	
	$\Gamma_3$	forbidden	—	—	—	—	—	—	—	—	—	
	$\Gamma_4$	$z$	D <sub>4</sub>	D <sub>3</sub>	D <sub>2</sub>	D <sub>1</sub>	D <sub>1</sub>	D <sub>1</sub>	D <sub>2</sub>	D <sub>2</sub>	D <sub>1</sub>	
With the spin-orbit interaction												
			D <sub>5</sub>	D <sub><i>i</i></sub> ( <i>i</i> = 2–5)		D <sub><i>i</i></sub> ( <i>i</i> = 3, 4)		D <sub><i>i</i></sub> ( <i>i</i> = 3, 4)				
$\Gamma_5$	$\Gamma_5$	$x, y, z$	D <sub>1</sub> + D <sub>2</sub> + D <sub>3</sub> + D <sub>4</sub>				D <sub>1</sub>	D <sub>1</sub> + D <sub>2</sub>		D <sub>1</sub> + D <sub>2</sub>		

the centre of the SLBZ and direct  $\Gamma$ – $\Gamma$  transitions are included in the figure. Energy levels corresponding to possible (in the case  $m + n = 2k$ ) folded band states and corresponding transitions involving these states are shown by dashed lines. Allowed polarizations of the transitions are indicated by corresponding arrows, polarizations allowed only due to the spin-orbit interaction in parentheses. In square brackets, the genesis of the band states is indicated, i.e. irreps of original states determining the distinct features of the band states are given. Since a group-theory analysis alone does not permit us to determine the energy positions of different band states, these diagrams could be specified on obtaining additional information from both band-structure calculations and experiments.

The analysis of the selection rules, results of band calculations, and the data of polarized-light optical experiments is to create the picture of electron-band structures of these superlattices. Studying the fine structure of the light-absorption spectra of high-quality SLs and comparing the oscillator strengths of lines in different polarizations one would obtain information of the nature of the lines (direct transitions and phonon-assisted ones) and evaluate the strengths of both spin-orbit and electron-phonon interactions.

**Table 15.** Selection rules and assisting phonons for indirect optical transitions in  $(\text{GaAs})_m(\text{AlAs})_n$  [111] SLs with the space group  $C_{3v}^1, C_{3v}^5$ .

Initial state (valence band)	Virtual state (conduction band)	Allowed polarizations	Final states							
			D = $\Gamma, A (C_{3v}^1)$		D = H, K ( $C_{3v}^1$ )			D = L, M ( $C_{3v}^1$ ) D = L, F ( $C_{3v}^5$ )		
			D = $\Gamma, T (C_{3v}^5)$		Without the spin-orbit interaction					
		D <sub>1</sub> D <sub>3</sub>		D <sub>1</sub> D <sub>2</sub> D <sub>3</sub>			D <sub>1</sub> D <sub>2</sub>			
			Assisting phonons							
$\Gamma_1$	$\Gamma_1$	$z$	D <sub>1</sub>	D <sub>3</sub>	D <sub>1</sub>	D <sub>2</sub>	D <sub>3</sub>	D <sub>1</sub>	D <sub>2</sub>	
$\Gamma_1$	$\Gamma_3$	$x, y$	D <sub>3</sub>	D <sub>1</sub> + D <sub>3</sub>	D <sub>2</sub> + D <sub>3</sub>	D <sub>1</sub> + D <sub>3</sub>	D <sub>1</sub> + D <sub>2</sub>	D <sub>1</sub> + D <sub>2</sub>	D <sub>1</sub> + D <sub>2</sub>	D <sub>1</sub> + D <sub>2</sub>
$\Gamma_3$	$\Gamma_1$	$x, y$	D <sub>1</sub>	D <sub>3</sub>	D <sub>1</sub>	D <sub>2</sub>	D <sub>3</sub>	D <sub>1</sub>	D <sub>2</sub>	
$\Gamma_3$	$\Gamma_3$	$x, y, z$	D <sub>3</sub>	D <sub>1</sub> + D <sub>3</sub>	D <sub>2</sub> + D <sub>3</sub>	D <sub>1</sub> + D <sub>3</sub>	D <sub>1</sub> + D <sub>2</sub>	D <sub>1</sub> + D <sub>2</sub>	D <sub>1</sub> + D <sub>2</sub>	D <sub>1</sub> + D <sub>2</sub>
			With the spin-orbit interaction							
			D <sub>4</sub>	D <sub>5</sub>	D <sub>6</sub>	D <sub>4</sub>	D <sub>5</sub>	D <sub>6</sub>	D <sub>3</sub>	D <sub>4</sub>
			Assisting phonons							
$\Gamma_4$	$\Gamma_5$	forbidden	—	—	—	—	—	—	—	—
	$\Gamma_4$	$z$	D <sub>3</sub>	none	D <sub>3</sub>	D <sub>3</sub>	D <sub>1</sub>	D <sub>2</sub>	D <sub>2</sub>	D <sub>1</sub>
	$\Gamma_6$	$x, y$	D <sub>1</sub>	D <sub>3</sub>	D <sub>1</sub> + D <sub>3</sub>	D <sub>1</sub> + D <sub>2</sub>	D <sub>2</sub> + D <sub>3</sub>	D <sub>1</sub> + D <sub>3</sub>	D <sub>1</sub> + D <sub>2</sub>	D <sub>1</sub> + D <sub>2</sub>
$\Gamma_5$	$\Gamma_5$	$z$	none	D <sub>1</sub>	D <sub>3</sub>	D <sub>3</sub>	D <sub>1</sub>	D <sub>2</sub>	D <sub>1</sub>	D <sub>2</sub>
	$\Gamma_4$	forbidden	—	—	—	—	—	—	—	—
	$\Gamma_6$	$x, y$	D <sub>1</sub>	D <sub>3</sub>	D <sub>1</sub> + D <sub>3</sub>	D <sub>1</sub> + D <sub>2</sub>	D <sub>2</sub> + D <sub>3</sub>	D <sub>1</sub> + D <sub>3</sub>	D <sub>1</sub> + D <sub>2</sub>	D <sub>1</sub> + D <sub>2</sub>
$\Gamma_6$	$\Gamma_5$	$x, y$	none	D <sub>1</sub>	D <sub>3</sub>	D <sub>3</sub>	D <sub>1</sub>	D <sub>2</sub>	D <sub>1</sub>	D <sub>2</sub>
	$\Gamma_4$	$x, y$	D <sub>3</sub>	none	D <sub>3</sub>	D <sub>3</sub>	D <sub>1</sub>	D <sub>2</sub>	D <sub>2</sub>	D <sub>1</sub>
	$\Gamma_6$	$x, y, z$	D <sub>1</sub>	D <sub>3</sub>	D <sub>1</sub> + D <sub>3</sub>	D <sub>1</sub> + D <sub>2</sub>	D <sub>2</sub> + D <sub>3</sub>	D <sub>1</sub> + D <sub>3</sub>	D <sub>1</sub> + D <sub>2</sub>	D <sub>1</sub> + D <sub>2</sub>

## 5. Conclusion

Summing up, the main results of this paper are as follows.

(i) The  $(\text{GaAs})_m(\text{AlAs})_n$  [110] SLs belong to three families specified by space groups  $C_{2v}^1, C_{2v}^7$ , and  $C_{2v}^{20}$  whereas the  $(\text{GaAs})_m(\text{AlAs})_n$  [111] ones constitute two families,  $C_{3v}^1$  and  $C_{3v}^5$ . In turn, depending on specific numbers of monolayers of materials constituting the unit cell, the crystal families described by  $C_{2v}^1, C_{2v}^{20}$ , and  $C_{3v}^1$  space groups are divided into subfamilies corresponding to non-equivalent atomic arrangements over the Wyckoff positions in the unit cell.

(ii) In contrast to [001] SLs, for [110] and [111] SLs, the rearrangement of atoms over the Wyckoff positions within each family is more subtle and results in variation of occupation of Wyckoff positions with the same site symmetry by atoms of the same type.

(iii) The symmetry of electronic band states at the symmetry points of the BZ and their dependence on SL period for a whole set of SLs was determined.

(iv) It was found that for the [111] SLs there is a splitting of  $\Gamma$  states due to the spin-orbit interaction in contrast to the [110] SLs where such splitting is absent. Moreover, with spin-orbit interaction being taken into account, all  $\Gamma$  states have the same symmetry in the [110] SLs.

(iv) The selection rules for direct and phonon-assisted optical transitions including the case when spin-orbit interaction is taken into account were established. We obtained a hierarchy of optical transitions, i.e. allowed, allowed due to spin-orbit interaction, and forbidden ones.

### Acknowledgments

The authors acknowledge an HTEC.CRG 960664 NATO grant. They are indebted to V P Smirnov for helpful discussions. One of them (AGP) wishes to thank the Ministère de l'Enseignement Supérieur et de la Recherche for its support.

### References

- [1] Kitaev Yu E, Panfilov A G, Tronc P and Evarestov R A 1996 *J. Phys.: Condens. Matter* at press
- [2] Popovic Z V, Cardona M, Richter E, Strauch D, Tapfer L and Ploog K 1989 *Phys. Rev. B* **40** 3040
- [3] Popovic Z V, Cardona M, Richter E, Strauch D, Tapfer L and Ploog K 1990 *Phys. Rev. B* **41** 5904
- [4] Kitaev Yu E and Evarestov R A 1988 *Fiz. Tverd. Tela* **30** 2970 (Engl. Transl. *Sov. Phys.-Solid State* **30** 1712)
- [5] Evarestov R A and Smirnov V P 1993 *Site Symmetry in Crystals: Theory and Applications (Springer Series in Solid State Sciences 108)* ed M Cardona (Heidelberg: Springer)
- [6] Gershoni D, Brener I, Baraff G A, Chu S N G, Pfeiffer L N and West K 1991 *Phys. Rev. B* **44** 1930
- [7] Schmid U, Christensen N E, Cardona M, Lukes F and Ploog K 1992 *Phys. Rev. B* **45** 3546
- [8] Kuan T S, Kuech T F, Wang W I and Wilkie E L 1985 *Phys. Rev. Lett.* **54** 201
- [9] Gomyo A, Suzuki T and Iijima S 1988 *Phys. Rev. Lett.* **60** 2645
- [10] Allen L T P, Weber R E, Wasburn J and Pao Y C 1987 *Appl. Phys. Lett.* **51** 670
- [11] Cloizeaux J 1963 *Phys. Rev.* **129** 554
- [12] Kovalev O V 1975 *Fiz. Tverd. Tela* **17** 1700 (Engl. Transl. *Sov. Phys.-Solid State* **17** 1106)
- [13] Zak J *Phys. Rev. B* **23** 2824
- [14] Evarestov R A and Smirnov V P 1984 *Phys. Status Solidi b* **122** 231, 559
- [15] Miller S C and Love W F 1967 *Tables of Irreducible Representations of Space Groups and Co-Representations of Magnetic Space Groups* (Boulder, CO: Pruett)
- [16] Bradley C J and Cracknell A P 1972 *The Mathematical Theory of Symmetry in Solids* (Oxford: Clarendon)
- [17] Hahn T (ed) 1983 *International Tables for Crystallography, vol A, Space Group Symmetry* (Dordrecht: Reidel)
- [18] Parmenter P G 1955 *Phys. Rev.* **100** 573